Defining static correction for jointly relocated earthquakes along the Blanco Transform Fault Zone based on SOSUS hydrophone data

Vincent S. Cronin, Baylor University
Department of Geology
P.O. Box 97354
Waco, TX 76798-7354
Vince_Cronin@baylor.edu

Keith A. Sverdrup, University of Wisconsin
Department of Geosciences
P.O. Box 413
Milwaukee, WI 53201
sverdrup@uwm.edu

***Abstract*–The Blanco Transform Fault Zone (BTFZ) is a complex ~350 km long segment of the boundary between the Pacific and Juan de Fuca plates, located ~200-500 km west of Point Blanco on the Oregon coastline. Individually located earthquake epicenters reported by the International Seismological Centre and the U.S. Geological Survey's National Earthquake Information Center along the BTFZ are not well correlated spatially with the active transform boundary due to poor azimuthal distribution of recording stations, inaccurate crustal velocity models or random reporting errors. More accurate locations of 120 m_b ≥ 5.0 earthquakes relative to each other have been obtained using the joint-relocation method of Jordan and Sverdrup [1, 2]. The Jordan-Sverdrup method simultaneously relocates epicenters in clusters of up to 20 events, yielding improved locations for epicenters within the cluster relative to each other. Six of the earthquakes in this set have been independently located using data from the U.S. Navy's SOSUS hydrophone array, enabling specification of a static correction to obtain improved absolute locations for the epicenters relative to the BTFZ. Of several methods evaluated, the preferred method to define the static correction in this case used the pole to the best-fit great circle through the six reference epicenters as one of two necessary fiducial points, and the projection of the largest earthquake onto the best-fit great circle as the other fiducial point. These fiducial points were used to define the rotation parameters for the static correction. The 95% confidence ellipses of the relocated epicenters generally fall on or very near active structural features along the BTFZ after application of the static correction.**

I. INTRODUCTION

It has been known for decades that the reported locations of individual earthquake epicenters along the Juan de Fuca ridge system, located teleseismically using body waves, do not coincide with the structures that generated them [3, 4]. The epicenters listed in the catalogs of the International Seismological Centre (ISC) [5] and U.S. Geological Survey's National Earthquake Information Center (NEIC) [6] are systematically mislocated toward the north or northeast of the active structures along the Blanco Transform Fault Zone (BTFZ) between the Pacific and Juan de Fuca plates (Fig. 1). The mislocations are due to the combined effects of the inadequate crustal velocity model that is routinely used, the poor azimuthal distribution of seismograph stations largely concentrated toward the northwest of the BTFZ, and random reporting errors [3, 4, 7, 8, 9].

In a companion study to be published elsewhere [2], we discuss the results of a joint relocation study we recently completed, involving 120 m_b ≥ 5.0 earthquakes reported near the BTFZ between 1964 and early 2003. The purpose of that study is to improve epicenter locations along the BTFZ so that the earthquakes can be better associated with active structures along the transform boundary, with the adjacent ridges, or with intra-plate deformation. The joint relocation method of Jordan and Sverdrup [1] is used to better locate the epicenters relative to each other. While this is the first published use of this method for earthquakes along the BTFZ, the Jordan-Sverdrup relocation method has been successfully used along other segments of the Juan de Fuca ridge system [10, 11, 12, 13] and elsewhere [1, 14].

Six of the earthquakes in our study set were also located using the U.S. Navy's SOSUS hydrophone array (Fig. 1), providing an opportunity to define a static correction with which the entire set of 120 relocated epicenters can be moved to bring them into better correspondence with active structures along the BTFZ. For convenience in illustration, the earthquakes are labeled with Greek letters as follows: α, m_b 6.2 event June 2, 2000; β, m_b 5.5 event November 4, 1996; χ, m_b 5.4 event April 15, 1996; δ, m_b 5.6 event October 27, 1994; ε, m_b 5.1 event January 19, 1994; and ϕ, m_b

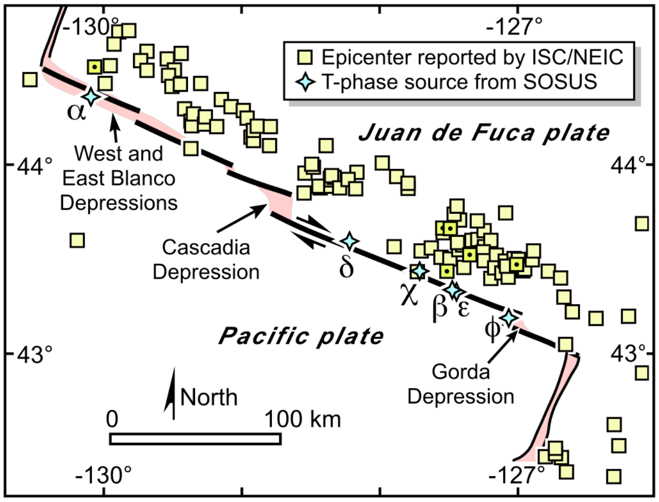

Fig. 1. Initial locations of epicenters from ISC or NEIC for 120 M≥5 earthquakes near the Blanco Transform Fault Zone. T-phase source locations for 6 reference earthquakes indicated by 4-point stars; corresponding 6 epicenters reported by ISC/NEIC indicated by squares containing black dots. Greek letter designations for reference epicenters are explained in the text.

5.1 event at 14:27Z on August 4, 1992 (Fig. 1) [15, 16, 17].

T-waves from each of the 6 earthquakes were detected in the SOFAR channel by 3-9 hydrophones in the SOSUS array, and the apparent source of the T-waves was resolved using a point-source model [17, 18, 19]. Within areas of the seafloor like the BTFZ, which is favorably located relative to the hydrophone array, the errors associated with T-wave source locations are typically smaller than the errors associated with epicenters located individually using body waves [20], although T-phase source locations are not always coincident with actual epicenters [21]. The SOSUS array provides a useful independent dataset for locating earthquakes.

The purpose of this paper is to provide a brief discussion of the methods we evaluated to define a static correction to bring a reference set of 6 relocated earthquake epicenters into appropriate spatial coincidence with the corresponding set of 6 epicenters determined using the SOSUS array. Details of the results are discussed elsewhere [2]; this paper is focused on the process of defining an appropriate static correction. The primary difficulty we encountered was the fact that the geometry of the 6 T-wave source locations defined by SOSUS was similar, but not identical, to the geometry of the 6 epicenters determined teleseismically using body waves (Fig. 1), so determination of a static correction was not simply a process of translating one set of epicenters to coincide with another geometrically identical set of epicenters.

II. INITIAL JOINT RELOCATION

The joint relocation method of Jordan and Sverdrup [1] simultaneously relocates earthquakes relative to each other in clusters of up to 20 events that occurred in proximity to one another. The set of 120 earthquakes along the BTFZ was divided into 12 overlapping clusters for relocation [2]. An example of three overlapping clusters of epicenters, as initially reported by the ISC or NEIC, is illustrated in Fig. 2. These clusters are located east of the Cascadia Depression and northwest of the Gorda Depression, and are of particular interest because they contain 4 of the 6 events that were also located using SOSUS data. (The epicenter symbols associated with these reference events are marked with black dots in Figs 1, 2 and 4.) Note that the SOSUS locations for these four events form a near-linear array in the following NW to SE order: □, □, □ and □ (Fig. 1). In contrast, the initial ISC/NEIC locations are not similarly aligned (Fig. 2).

Events □, □ and □ were each relocated in two clusters, resulting in 2 relocated epicenters per event (Fig. 3). For each of these three events (and indeed for all 20 events relocated as part of 2 of these particular 3 clusters), the 95% confidence interval (CI) error ellipses for the two solutions overlap one another. In a similar manner, the resulting error ellipses overlapped for more than 80% of the 65 events relocated in more than one cluster throughout the set of 120 earthquakes studied, leading us to assert that each epicenter relocated in the study is better located relative to every other relocated epicenter. When a given earthquake was relocated in more than one cluster, we considered the result with the smaller error ellipse to be the preferred result (*i.e.,* the result that was carried forward to the next step in the analysis).

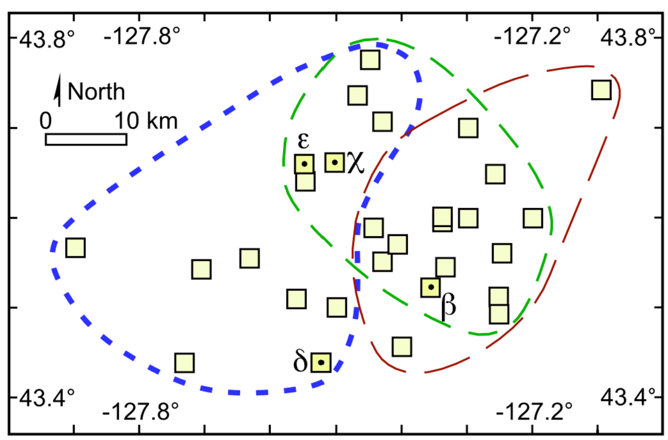

Fig. 2. Three clusters (enclosed by dashed curves) defined using initial locations of epicenters (squares) from ISC or NEIC for 29 M≥5 earthquakes near the Blanco Transform Fault Zone. Four reference events for which T-phase source locations are available indicated by squares containing black dots. Greek letter designations for reference epicenters are explained in the text.

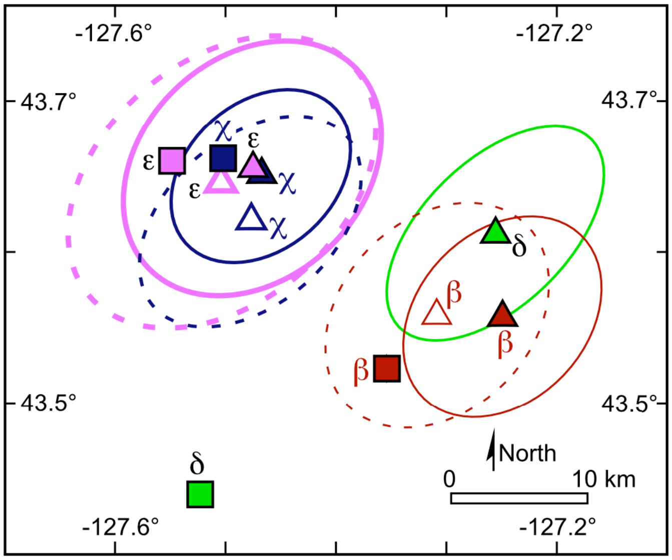

Fig. 3. Effect of cluster relocation of epicenters for four reference events. Greek letter designations for reference epicenters are explained in the text. Initial ISC/NEIC locations are squares. Results of cluster relocations are triangles. Filled triangles and solid 95% CI error ellipses indicate relocated epicenters with smaller error ellipses that were used in subsequent static correction; open triangles and dashed ellipses indicate solutions with larger error ellipses that were not used.

After relocation, the epicenters for the reference events in Fig. 3 formed a much more linear array in the following NW-to-SE order: □, □, □and □. The spatial order after relocation was still not the same as the spatial order of the SOSUS-derived T-wave source location for these events (*cf.* Figs. 1 and 3).

Relocation of all 29 events in the three clusters shown in Fig. 2 resulted in a tighter, more elongate zone of epicenters (Fig. 4). The epicenters after joint relocation are better located relative to each other, but are still not well located relative to the active structures along the BTFZ thought to have generated the earthquakes. There was no apparent relationship between the distance between the original and relocated epicenter versus either the magnitude of the earthquake or the number of reported arrivals. In contrast, there was a strong relationship between the size of the error ellipse and the number of reported arrivals (Fig. 5). All of the events whose 95% CI error ellipses exceeded 1,120 km^2 in area were reported by <50 stations, generally reflecting weaker or older events. The axial ratios of the error ellipses were rather consistent, averaging 1.9±0.5, so it was appropriate to directly compare ellipse areas.

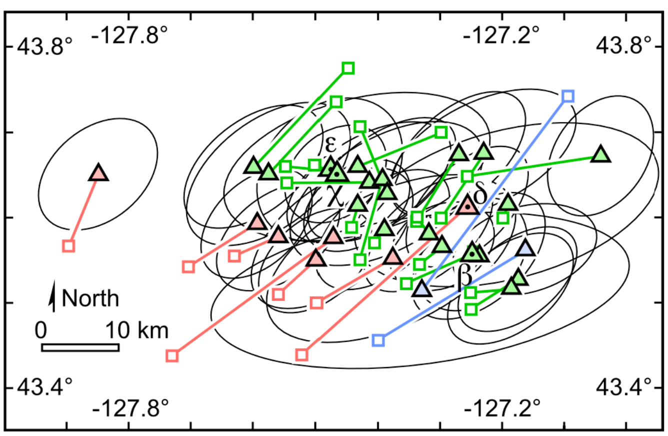

Fig. 4. Effect of cluster relocation of epicenters for 29 events in 3 clusters shown in Fig. 2. Initial epicenter locations are open squares. Relocated epicenters are triangles, shown with 95% CI error ellipses. Four reference epicenters are indicated with black dots. Greek letter designations for reference epicenters are explained in the text.

III. STRATEGIES FOR DEFINING STATIC CORRECTION

We evaluated four general strategies for using T-wave source locations from SOSUS to define a static correction to bring the relocated set of 120 epicenters into better spatial correspondence with active structures along the BTFZ. The first strategy was developed when we were initially aware of only one independent T-phase source location that correlates with an event in our study set: event □, which is also the strongest earthquake in our study [15, 17, 20]. Arnot and others [22] defined a pole of rotation using the unitized vector result of the cross product

$$\boldsymbol{P}_{\square} = \boldsymbol{S}_{\square} \times \boldsymbol{J}_{\square}, \qquad (3.1)$$

where $\boldsymbol{S}_{\square}$ is the unit location vector to the T-phase source location for event □, $\boldsymbol{J}_{\square}$ is the vector to the joint-relocation result for event □, and $\boldsymbol{P}_{\square}$ is the rotational pole around which $\boldsymbol{J}_{\square}$ can be moved along a great circle to coincide with $\boldsymbol{S}_{\square}$. After defining the vector angle □ between $\boldsymbol{S}_{\square}$ and $\boldsymbol{J}_{\square}$, the 120 relocated epicenters were rotated as a rigid set by □ around $\boldsymbol{P}_{\square}$. The result was a significant improvement in spatial coincidence between

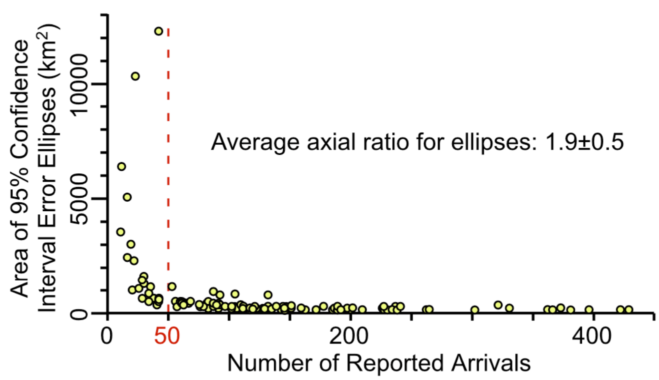

Fig. 5. Area of 95% CI error ellipses as a function of number of reported arrivals for 120 events. All of the events with large error ellipses (>1120 km^2) are located by < 50 arrivals.

the relocated epicenters and the BTFZ; however, the epicenters on the southeastern end of the BTFZ were still located slightly north of the active structures. This divergence probably resulted from the one-dimensional character of the static correction, based on the linear (great-circle) translation of $\boldsymbol{J}_{□}$ to coincide with $\boldsymbol{S}_{□}$.

Other strategies were developed when additional published T-phase source locations for events in our study became known to us [16]. The second strategy involved separate static corrections for each cluster that contained events that had also been located using SOSUS. Some of the events included in these initially repositioned clusters had also been relocated as part of other clusters that lacked SOSUS-located events. By aligning epicenters relocated in multiple clusters, it should be possible to integrate the clusters that do not include SOSUS-located events with those that *do*, for the purpose of completing the static correction.

One problem in implementing this strategy is that the geometry of the T-phase source locations is different in some cases than the geometry of the corresponding relocated epicenters, even within a single cluster. For example, the T-phase source locations indicate that three specific events occurred in the following order along a northwest-to-southeast line: □, □ and □ (Fig. 1). These same events were relocated within a common cluster and formed a similar northwest-to-southeast line, but the relocated epicenters are in a different order: □, □ and □ (Figs. 3 and 4). While a number of *ad hoc* solutions to this ordering discrepancy can be imagined, there was no obvious and reasonable way to handle this problem.

There is a second, more critical, problem with the second strategy. Moving individual clusters that contain one or more reference epicenters, so that they coincide better with the corresponding T-phase source locations, has the undesirable effect of moving those particular clusters *relative to each other*. Consequently, it was difficult to fit the remaining clusters that did not contain SOSUS-located events back together with the clusters that *did* have SOSUS-located events. The interlocking puzzle pieces, spatially related to one another by way of the events relocated in more than one cluster, no longer fit together well. We concluded that this strategy tended to partially negate the benefit of the initial relocation procedure, which had better located the epicenters relative to each other.

The third strategy sought to take advantage of the near-linear geometry of both groups of 6 independently located reference events (Fig. 6). Leonhard Euler first noted *circa* 1776 that if the location of two points are known in each of two rigid sets of points on a sphere, and those two points are the same angular distance apart in both sets, then an axis can be uniquely defined around which the fiducial points can be rotated into coincidence with one another.

Let $\boldsymbol{A}_1$ and $\boldsymbol{B}_1$ be the unit location vectors to fiducial points for rigid set 1, and $\boldsymbol{A}_2$ and $\boldsymbol{B}_2$ are unit vectors to fiducial points for set 2, such that all points are on a unit sphere and the angular distance between $\boldsymbol{A}_1$ and $\boldsymbol{B}_1$ is the same as the angle between $\boldsymbol{A}_2$ and $\boldsymbol{B}_2$. The unit location vector ($\boldsymbol{P}_{AB}$) to the pole around which $\boldsymbol{A}_1$ and $\boldsymbol{B}_1$ can be rotated to bring them into coincidence with $\boldsymbol{A}_2$ and $\boldsymbol{B}_2$ is given by

$$\boldsymbol{P}_{AB} = ((\boldsymbol{A}_1 \times \boldsymbol{A}_2) \times \boldsymbol{M}_A) \times ((\boldsymbol{B}_1 \times \boldsymbol{B}_2) \times \boldsymbol{M}_B), \quad (3.2)$$

where $\boldsymbol{M}_A$ is the midpoint between $\boldsymbol{A}_1$ and $\boldsymbol{A}_2$, and $\boldsymbol{M}_B$ is the midpoint between $\boldsymbol{B}_1$ and $\boldsymbol{B}_2$. The rotation angle necessary to bring $\boldsymbol{A}_1$ and $\boldsymbol{B}_1$ into coincidence with $\boldsymbol{A}_2$ and $\boldsymbol{B}_2$ is given by

□ = □ / sin(□), (3.3)

where □ is the angle between $\boldsymbol{P}_{AB}$ and $\boldsymbol{A}_1$ and □ is the angle between $\boldsymbol{A}_1$ and $\boldsymbol{A}_2$.

We initially used the pole to the best-fit great circle through the 6 epicenters as one fiducial point, and the average location vector for the 6 epicenters as the second fiducial point (Fig. 6). The best-fit great circle was defined using a least-squares criterion. An initial trial pole was defined by taking the cross product of the location vectors to the epicenters for events □ and □, which are on opposite ends of the array. Other trial poles were evaluated in an iterative manner within a geographic area around that initial location. The orientation tensor technique [23, 24] is an alternative method for defining the best-fit great circle. The average location vectors were defined by unitizing the vector sum of all 6 location vectors associated with each set of reference epicenters. No weighting factors were used in computing the average or defining the best-fit great circle.

After rotation, the best-fit great circle and average location vector associated with the 6 reference epicenters in the set of relocated earthquakes were coincident with those associated with the 6 T-phase source locations for the same earthquakes (Fig. 6b). The result was considered a mixed success. While the relocated epicenters for events □ and □ were nearly coincident with the T-phase source locations for those same events, the SOSUS source locations were not within the 95% CI error ellipses of the relocated earthquakes for events □, □, □ or □. In particular, the relocated epicenter for events □ and □ seemed to be mislocated to the northwest of their expected locations. This is because relocated epicenters □, □, □, □ and □ are bunched together within 50 km of each other, while the corresponding T-phase source locations are distributed over more than twice the distance. The effect of this difference is that the average location of the relocated epicenters is skewed away from the relocated epicenter for event □, compared with the average for the T-phase source locations, shifting all of the relocated epicenters too far northwest after static correction (Fig. 6b).

Another indicator that the third strategy was not optimal is the distribution of foreshocks and aftershocks

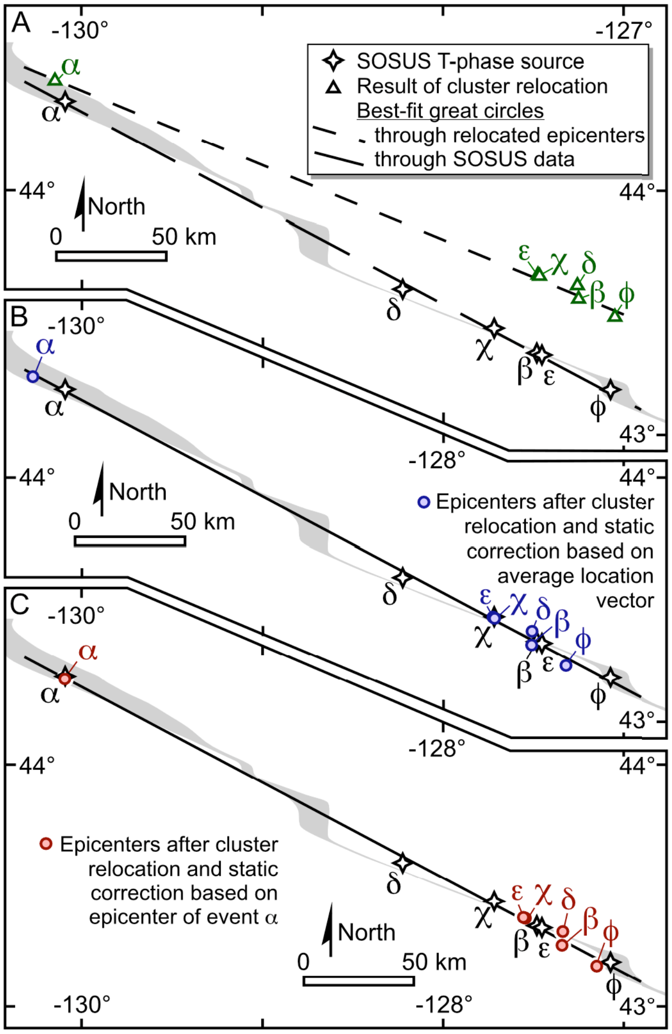

Fig. 6. Strategies for defining static correction. (A) Initial configuration. (B) Result of strategy 3, using average epicenter locations as fiducial points. (C) Result of strategy 4, using projections of event □ onto best-fit great circle as fiducial points. Greek letter designations for reference epicenters are explained in the text.

from event □ [15, 17, 20]. The locations of these smaller events make geologic sense if they occurred as indicated by their T-phase source locations: throughout the West Blanco Depression. If the main earthquake actually occurred where the relocated epicenter for event □ was projected after static correction, the associated minor events would extend to the northwest out of the basin and beyond the southern tip of the Juan de Fuca ridge. It seemed more likely that the third strategy had not yielded an optimal location for event □ after static correction.

The fourth strategy utilized the same general approach as the third strategy; however, instead of using the average location of all 6 reference events to establish one of the two necessary fiducial points (along with the pole to the best-fit great circle), the fourth strategy used the projection of the epicenter for event □ onto the best-fit great circle. Let us define unit location vector ***P*** as the pole to the best-fit great circle through the 6 reference events, $\boldsymbol{S}_{\square}$ is the unit location vector to epicenter □, and $\boldsymbol{V}_{\square}$ is the projection of $\boldsymbol{S}_{\square}$ onto the best-fit great circle. Then $\boldsymbol{V}_{\square}$ is given by

$$\boldsymbol{V}_{\square} = \boldsymbol{P} \times (\boldsymbol{S}_{\square} \times \boldsymbol{P}). \qquad (3.4)$$

The fourth strategy yielded overlapping 95% CI error ellipses for 4 of the 6 reference events: □, □, □ and □ (Fig. 6c). The 95% CI error ellipses for event □ were within ~10 km of each other, while the T-phase source location for event □ diverged from the corresponding relocated epicenter by a significant amount (> 70 km). A model that would result in additional migration of the relocated epicenters toward the southeast would initially improve the fit for events □ and □, but would worsen the correlation for events □, □, □ and □.

The fourth strategy for defining a static correction resulted in specification of rotation parameters needed to move the 120 relocated epicenters as a rigid vector set to their final improved locations along the BTFZ. The 95% confidence ellipses of the relocated epicenters typically fall on or very near active structural features along the BTFZ after the static correction is applied [2].

IV. CONCLUSIONS

Teleseismically recorded earthquakes along the BTFZ are routinely mislocated toward the north and east. The joint-relocation procedure of Jordan and Sverdrup [1] results in improved location of epicenters along the BTFZ relative to each other; however, the relocated epicenters did not coincide with active plate-boundary structures [2]. Recent availability of T-phase source locations associated with earthquakes that have also been recorded teleseismically has allowed us to specify a static correction to improve relocation of historic earthquakes along the BTFZ. Use of the T-phase source locations for 6 reference earthquakes was complicated by the fact that the geometry of these source locations was broadly similar, but not identical, to the geometry of the corresponding 6 relocated epicenters. In this study, the preferred method to define the static correction used the pole to the best-fit great circle through the reference epicenters as one of two necessary fiducial points, and the projection of the largest earthquake onto the best-fit great circle as the other fiducial point. Defining two comparable points in both the set of relocated epicenters and the set of T-phase source locations allowed specification of rotation parameters needed to bring those points into coincidence, thus defining a static correction for the relocated epicenters.

Acknowledgments

We thank J.M. Arnot, A.S. Ledger, M.L. Perkins, S. Ruddock, B.J. Salentine, S.J. Salentine, and H.E. Larsen for their work on the initial phases of this project.

References

[1] T.H. Jordan and K.A. Sverdrup, “Teleseismic location techniques and their application to earthquake clusters in the south-central Pacific,” *Bull. Seismol. Soc. Am.*, vol. 71, pp. 1105-1130, 1981.

[2] V.S. Cronin and K.A. Sverdrup, “Multiple-event relocation of historic earthquakes along the Blanco Transform Fault Zone, NE Pacific,” unpublished.

[3] J. Northrop, H.W. Menard and F.K. Duennebier, “Seismic and bathymetric evidence of a fracture zone on Gorda Ridge,” *Science*, vol. 161, pp. 688-690, 1968.

[4] J. Northrop, “Accuracy of earthquake epicenters on the Gorda ridge,” *Bull. Seismol. Soc. Am.*, vol. 60, pp. 265-267, 1970.

[5] International Seismological Centre, “On-Line Bulletin,” http://www.isc.ac.uk/Bull, 2003.

[6] National Earthquake Information Center, “Data files available through FTP,” http://neic.usgs.gov/neis/data_services/ftp_files.html, 2003.

[7] S.H. Johnson and P.R. Jones, “Microearthquakes located on the Blanco fracture zone with sonobuoy arrays,” *J. Geophys. Res.*, vol. 83, pp. 255-261, 1978.

[8] P.R. Jones and S.H. Johnson, “Sonobuoy array measurements of active faulting on the Gorda Ridge,” *J. Geophys. Res.*, vol. 83, pp. 3435-3440, 1978.

[9] E.A. Bergman and S.C. Solomon, “Transform fault earthquakes in the North Atlantic: Source mechanism and depth of faulting,” *J. Geophys. Res.*, vol. 93, pp. 9027-9057, 1988.

[10] K.A. Sverdrup, “Multiple-event relocation of earthquakes on and near the Gorda Ridge,” *Geophys. Res. Lett.*, vol. 13, pp. 674-677, 1986.

[11] K.A. Sverdrup, “Multiple-event relocation of earthquakes near the Gorda Rise-Mendocino Fracture Zone intersection,” *Geophys. Res. Lett.*, vol. 14, pp. 347-350, 1987.

[12] P.R. Stoddard and M.T. Woods, “Master event relocation of Gorda block earthquakes: Implications for deformation,” *Geophys. Res. Lett.*, vol. 17, pp. 961-964, 1990.

[13] D.J. Bebel, P.R. Stoddard and M.T. Woods, “A comparison of epicenter relocation techniques: A case study for the Juan de Fuca plate,” *Phys. Earth and Planet. Int.,* vol. 75, pp. 25-38, 1992.

[14] K.A. Sverdrup, G.J. Schurter, and V.S. Cronin, “Relocation analysis of earthquakes near Nanga Parbat-Haramosh Massif, northwest Himalaya, Pakistan,” *Geophys. Res. Lett.*, vol. 21, pp. 2331-2334, 1994.

[15] C.G. Fox, R.P. Dziak and P. Will, “Seismic activity – western Blanco Transform Fault: June 2-3, 2000,” http://www.pmel.noaa.gov/vents/acoustics/seismicity/nepac/wbfz0600.html, 2000.

[16] R.P. Dziak, C.G. Fox, R.W. Embley, J.L. Nabelek, J. Braunmiller and R.A. Koski, “Recent tectonics of the Blanco Ridge, eastern Blanco Transform Fault Zone,” *Mar. Geophys. Res.*, vol. 21, pp. 423-450, 2000.

[17] R.P. Dziak, W.W. Chadwick, Jr., C.G. Fox and R.W. Embley, “Hydrothermal temperature changes at the southern Juan de Fuca Ridge associated with a Mw 6.2 Blanco Transform earthquake,” *Geology*, vol. 31, pp. 119-122, 2003.

[18] P.D. Slack, C.G. Fox, and R.P. Dziak, “P-wave detection thresholds, Pn velocity estimates, and T-wave location uncertainty from oceanic hydrophone arrays,” *J. Geophys. Res.*, vol. 104, pp. 13,061-13,072, 1999.

[19] C.G. Fox, R.P. Dziak, H. Matsumoto and A.E. Schreiner, “Potential for monitoring low-level seismicity on the Juan de Fuca Ridge using fixed hydrophone arrays,” *Mar. Tech. Soc. J.,* vol. 27, pp. 22-30, 1994.

[20] D.W. Bohnenstiehl, M. Tolstoy, R.P. Dziak, C.G. Fox, and D.K. Smith, “Aftershock sequences in the mid-ocean ridge environment: An analysis using hydroacoustic data,” *Tectonophys.*, vol. 354, pp. 49-70, 2002.

[21] C.G. Fox, H. Matsumoto and T.-K.A. Lau, ”Monitoring Pacific Ocean seismicity from an autonomous hydrophone array,” *J. Geophys. Res.*, vol. 106, pp. 4183-4206, 2001.

[22] J.M. Arnot, A.S. Ledger, M.L. Perkins, S. Ruddock, B.J. Salentine, S.J. Salentine, H.E. Larsen, III, V.S. Cronin and K.A. Sverdrup, 2001, “Multiple-event relocation of Blanco Transform Fault Zone earthquakes,” *Eos Trans. Am. Geophys. Union*, vol. 82(47), p. F1118, 2001.

[23] N.I. Fisher, T. Lewis and B.J.J. Ebleton, 1987, *Statistical analysis of spherical data*. New York: Cambridge University Press, 1987, 329 pp.

[24] D.S. Wilson, “Confidence intervals for motion and deformation of the Juan de Fuca plate,” *J. Geophys. Res.*, vol. 98, pp. 16,053-16,071, 1993.